Si nanoclusters coupled to Er^{3+} ions in a SiO$_2$ matrix for optical amplifiers

D. Navarro-Urrios [a,*], O. Jambois [a], F. Ferrarese Lupi [a], P. Pellegrino [a], B. Garrido [a], A. Pitanti [b], N. Prtljaga [b], N. Daldosso [b], L. Pavesi [b]

[a] MIND-IN2UB, Dept. Electrònica, Universitat de Barcelona, Martí i Franquès 1, 08028 Barcelona, Spain
[b] Laboratorio di Nanoscienze, Dipartimento di Fisica, Università di Trento, Via Sommarive 14, I-38100, Povo (Trento), Italy

ARTICLE INFO

ABSTRACT

In this work we will give an overview of the optical properties of Si nanoclusters coupled to Er^{3+} ions in SiO$_2$ matrices produced by reactive magnetron co-sputtering. We have divided the work into two separate studies realised on the same samples, which are the result of a thorough optimisation work. The first one have been realised in order to get a clear picture of the interaction mechanism. On the second we will show a quantitative evaluation of the potential performances from a material point of view (determination of the whole optically active Er^{3+} content, excitable by direct or indirect means) and actual performance in a waveguide device (determination of internal gain values).

© 2010 Elsevier B.V. All rights reserved.

1. Introduction

One of the scientific and technological challenges of silicon-based photonics consists in making silicon an efficient light emitter, eventually also providing amplification. This will allow combining both the functionality of silicon microelectronics with ultra-fast optical data generation, processing and transmission on a single silicon-based device.

Low dimensional silicon in the form of silicon nanoclusters (Si-nc) is a material with extremely interesting optoelectronic properties that differ strongly from those of bulk Si. In particular, the capacity of Si-nc to act as sensitizers of rare earth ions, specifically erbium ions (Er^{3+}) [1], has opened the route towards an all-optical light Si based amplifiers operating in the third telecommunication window. However, during the last years, several reports have shown what seems to be an intrinsic limit of the material itself, as to say. the low amount of Er^{3+} taking advantage of an efficient indirect transfer mechanism [2–5]. The fundamental reason of the low excitable percentage is still under debate and a number of different issues have been proposed as final limiting factors. Among them, the most extended ones have been the finite interaction distance of the coupling strength [4], the presence of Auger back-transfer mechanisms [5], excited state absorption processes [6] cooperative up-conversion [3] and the limited concentration of Er^{3+} ions able to emit light [7].

The study presented here is crucial for the understanding and optimisation of the performances of this material, which has been in this case fabricated by reactive magnetron co-sputtering.

In the first part of the paper we will show a modelling of the transfer mechanism through a set of coupled rate equations involving the carrier populations of a number of effective levels within the Si-nc and the Er^{3+} ions. This model includes several recombination and excitation mechanisms, well grounded on the basis of several evidences observed in continuous wave and time-resolved photoluminescence measurements. We will address afterwards the issue of quantifying of the different concentrations that determine the potentiality of the material for light amplification, as to say: (i) the total content of erbium present in the material, (ii) the concentration of Er^{3+} ions that are absorbing light, (iii) the concentration of the ones that are optically active and emit light, (iv) the concentration of the ones that are efficiently coupled to the Si-nc and emit light.

Finally, the characterisation will be addressed of waveguide devices that quantify absolute values of absorption losses and gain.

2. Experimental

The samples under study have been fabricated by a RF reactive magnetron co-sputtering under Argon–Hydrogen mixture of 2-in. confocal pure SiO$_2$ and Er$_2$O$_3$ targets [8]. To form nanoparticles, a substoichiometric Silicon Rich Silicon Oxide (SRSO) has been deposited followed by an annealing treatment to promote phase separation between silicon and its oxide. In order to perform comparative spectroscopic characterisation, the deposition parameters

* Corresponding author.
  E-mail address: dnavarro@el.ub.es (D. Navarro-Urrios).

employed to obtain the best sample in terms of high PhotoLumi-nescence (PL) intensity (under non-resonant pumping – 476 nm) and long lifetime of the $^4I_{13/2} \rightarrow {}^4I_{15/2}$ Er^{3+} transition, have been used to fabricate a set of different samples with and without Er^{3+} and with different annealing treatments.

Here we will report about two samples deposited over a 5 μm-SiO$_2$ cladding layer above a Si substrate: sample A (Si excess of 5%, Er^{3+} content of 3.4×10^{20} cm^{-3}, and thickness 1.2 μm) and sample B (same deposition conditions but without Er^{3+}). Both layers were annealed at 910 °C during 60 min under a pure nitrogen flow, so they likely contain Si in an amorphous nanocluster form [8]. Some of the measurements shown in this paper were done on rib-loaded waveguides, which have been formed by dry etching the slab waveguides [9].

The spectroscopic experiments have been performed both in visible (VIS) and near-infrared (IR) range, with Continuous-Wave (CW) and pulsed laser excitation sources. The CW source was an Ar$^+$ laser of which we have employed lines which were resonant (488 nm) or non-resonant (476 nm) with Er^{3+} internal transitions.

The pulsed source was the third harmonic (355 nm) of a Nd:YAG laser with 10 ns pulse width, a repetition rate of 10 Hz and a photon flux of 1×10^{25} ph/(cm^2 s) during the pulse. For detection in the visible we have used a CCD streak camera coupled to a spectrometer, with an overall time-resolution of the order of few picoseconds, and a monochromator coupled with a GaAs-PhotoMulTiplier (PMT), respectively for Time Resolved (TR) and CW measurements. In the infrared, the signal was spectrally resolved with a monochromator and subsequently detected with a InGaAs IR-PMT. All measurements have been performed at room temperature.

3. Results

A typical PL spectrum of our samples, measured with an excitation wavelength non-resonant with any Er^{3+} internal transition (476 nm), is shown in Fig. 1. It is possible to recognize several spectral features: around 980 nm and 1535 nm, the characteristic transitions of Er^{3+} in SiO$_2$ appear, related respectively to the first and second excited to the fundamental state optical transitions. The

wide band centred at around 700 nm is related to Si-nc emission, while the emission band at about 1100 nm is due to the Si sub-strate. In the right panels of the same figure we present separately the temporal decay of the PL signals after a fast (10 ns) pulsed excitation at 355 nm for the IR transitions (top right), related to Er^{3+} emission, and for the VIS transitions (bottom right), related to Si-nc emission.

The analysis of the IR emission reveals that the signal at 0.98 μm ($^4I_{11/2} \rightarrow {}^4I_{15/2}$ transition) after a steep rise that lasts less than 100 ns is constantly decreasing as a single exponential function, with a time constant of 4.6 ± 0.5 μs. On the other hand, the 1.535 μm signal ($^4I_{13/2} \rightarrow {}^4I_{15/2}$ transition) is rising with almost the same time constant (4.2 ± 0.5 μs). It is not possible to compare directly the populations in the two levels, since the PL intensities are inversely proportional to the unknown radiative lifetimes. However, it is clear that the 1.535 μm signal never rises above the 0.98 μm one, implying that a great part of the energy transfer process involves the level $^4I_{11/2}$ and that the level $^4I_{13/2}$ is populated mainly through internal relaxation processes. A fast transfer process that populates directly the $^4I_{13/2}$ level could be also present, though its impact would be at most of the same magnitude than the transfer to the $^4I_{11/2}$ level. It is not possible to exactly quantify its contribution since the first nanoseconds of PL dynamics are hidden by a fast decaying emission that will be discussed hereafter.

The single exponential function observed in the 0.98 μm decay suggests that no level energetically higher than $^4I_{11/2}$ is excited during the transfer process, since otherwise the $^4I_{11/2}$ would be repopulated during the decay, at least during the first tens of ns. This is further supported by the absence of visible PL emission involving transitions from higher energy levels.

One of the most striking features is the appearance of a very fast (tens of ns) signal, already mentioned in the previous discussion. A similar component was observed by other authors and was associated to Auger back-transfer mechanisms from excited Er^{3+} to excited carriers within the Si-nc [5], however it covers a very broad spectral range, i.e. not only where Er^{3+} transitions are present [10,11]. Moreover, the same kind of fast component is present also for sample B, whose intensity of the visible PL is quenched by roughly the same factor when erbium is inserted in the sample (see next paragraphs). Its origin could be attributed to radiative
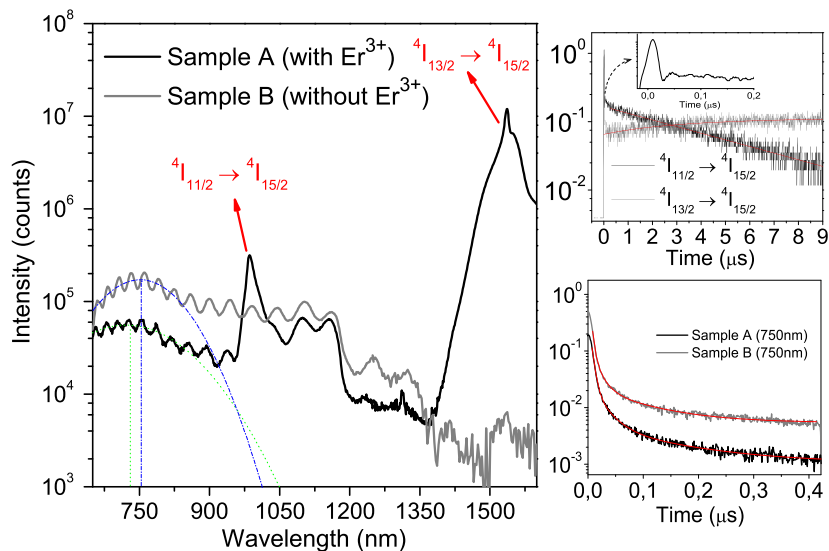

Fig. 1. PL emission from sample A (black) and B (gray). Gaussian fits to the Si-nc associated emission have been included. The top right panel shows a comparison of $^4I_{11/2} \rightarrow {}^4I_{15/2}$ and $^4I_{13/2} \rightarrow {}^4I_{15/2}$ PL temporal behaviours after the pump pulse in sample A. In red, the simulation results using the model presented in this manuscript are reported, holding a decay time of 4.6 ± 0.5 μs (980 nm signal) and a rise time of 4.2 ± 0.5 μs (1535 nm signal). A zoom of the first 200 ns for the PL associated to the $^4I_{11/2} \rightarrow {}^4I_{15/2}$ has been also included. The bottom right panel shows the experimental and simulated (red curves) PL decays of the visible signal (0.65–0.95 μm). (For interpretation of the references to color in this figure legend, the reader is referred to the web version of this article.)

emitting centres related to Si-nc, as the ones reported in Ref. [11]. However, most importantly is that it cannot be attributed to back-transfer related dynamics.

Respect to sample B the CW measurement reveals that the PL of sample A in the visible region is quenched as a whole, without showing any apparent spectral features. This decrease is only about a factor of 3, so a clear residual VIS-PL emission is still present in the sample with Er^{3+}. Since the intrinsic recombination lifetime for excitons within Si-nc is of the order of tens of μs, in a case of a transfer mechanism related to interband recombination, the energy transfer to Er^{3+} would be expected to be quite inefficient, which is not the case.

When Er^{3+} ions are introduced in the sample, also the VIS-PL lifetime gets reduced. However, the PL decay only speeds up for sample A during the first tens of ns as a consequence of the transfer process, while afterwards the temporal evolution of the PL signal is roughly the same (although lower in intensity). Actually, the decay of sample B can be divided in two parts: (i) a slow process with a stretched exponential line shape (tens to hundreds of μs) that is typical of the spontaneous emission process in Si-nc; and (ii) a fast decay (tens of ns) that is associated to Auger recombination mechanisms within the Si-nc. This latter statement is further supported by CW–PL measurements, where the intensity has a sublinear dependence with the pump power. In fact, in the case of sample B the power coefficient is very close to 2/3, which is the signature of a three particle Auger recombination mechanism [12]. Although sample B is more intense, the power coefficient is larger for sample A (about 0.83).

A detailed model of the electronic and optical properties of a single Si-nc can only be built with extreme difficulty. Moreover, due to the specific deposition characteristics of the studied samples the most probable situation is that, within the active material, an ensemble of Si-nc of different sizes and geometries is present. For this reason, we have modelled the dynamics of the system by a phenomenological set of rate equations. A simplified description of the system allows simulating the overall experimental picture described in the previous paragraphs. It is worth to note that this model is valid only for the first hundreds of nanoseconds after the excitation, where Auger and the transfer mechanism dominate the dynamics of the carriers within the Si-nc (intrinsic and bimolecular-like recombination mechanisms are neglected) and, consequently, the Er^{3+} excitation.

In this scheme (see Fig. 2), a Si-nc is represented by an effective three level system (which could be constituted by manifolds), consisting of two band edge levels that account for the fundamental ground state (Ex1) and the radiative level that originates the PL emission (Ex2) and high-lying level which absorbs the incoming 355 nm radiation (Ex3).

On the other hand Er^{3+} is schematized as a three levels system: $^4I_{11/2}$, $^4I_{13/2}$ and $^4I_{15/2}$.

$$\frac{d}{dt}N_{exc,1} = -\sigma_{Si\text{-}np}\Phi_{exc}(t)N_{Si\text{-}np} + 0.5C_A(N_{exc,2})^3$$

$$\frac{d}{dt}N_{exc,2} = \omega_{32}N_{exc,3} - C_A(N_{exc,2})^3$$

$$\frac{d}{dt}N_{exc,3} = \sigma_{Si\text{-}np}\Phi_{exc}(t)N_{Si\text{-}np} - 0.5C_A(N_{exc,2})^3$$

$$\frac{d}{dt}N_{Er,1} = -kN_{exc,3}N_{Er,1} + 1/\tau_{21}N_{Er,2} \qquad (1)$$

$$\frac{d}{dt}N_{Er,2} = 1/\tau_{32}N_{Er,3} - 1/\tau_{21}N_{Er,2}$$

$$\frac{d}{dt}N_{Er,3} = kN_{exc,3}N_{Er,1} - 1/\tau_{32}N_{Er,3}$$

- $\sigma_{Si\text{-}nc}$, (t) and C_A are, respectively, the Si-nc absorption cross section ($\sim 1 \times 10^{15}$ cm²), Φ the pump flux (temporal shape as the experimental pulse) at excitation wavelength (355 nm) and the Auger coefficient.
- ω_{ij} is the probability of the $i \to j$ transitions while τ_{ij} is the inverse of the transition probability.
- k is the coupling constant for the energy transfer process among Si-nc an Er ions. As reported in different works, the coupling constant scales with distance following an exponential decay, which is typical of a Dexter-like transfer process [4,13]. In this kind of interaction mechanism any energy transfer event is given by an electronic exchange between the donor (electron in Si-nc) and acceptor (electron in the $^4I_{15/2}$ level of an Er^{3+} ion) due to a partial overlap of their initial wavefunctions.

Once an exciton has been formed in level Ex3 it can relax either to level Ex2 or to an internal effective-trap-state transferring the energy difference to an Er^{3+} nearby, which gets excited. If relaxation to level Ex2 occurs, the carrier can be re-excited back to level Ex3 by an Auger or alternatively can radiatively recombine to the level Ex1, emitting photons responsible for the Si-nc emission band reported in Fig. 1. Thus, Auger mechanisms could be considered more as a feedback than a detrimental process.

The existence of a "trap-like" state through which the Si-nc could sensitize Er^{3+} ions has been postulated in the literature, with strong direct experimental evidences recently obtained for Er^{3+} doped bulk Si [14]. This state is assumed in the model as an effective level (correlated with the presence of Si-nc in the matrix). The existence of an effective trap level explains the decrease of the whole VIS-PL spectra when Er ions are introduced in the SRO matrix.

It is worth to note that a good selection of the different parameters (keeping the values related with experimental constraints)
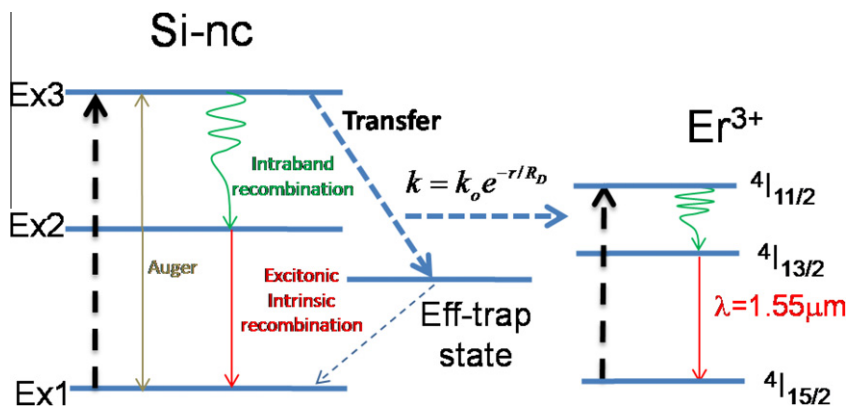

Fig. 2. Scheme of the levels and transitions involved in the transfer mechanism.

allows reproducing the experimental dynamics of both samples just by "switching on" the transfer mechanism. More details on the modelling can be found elsewhere [15].

When performing measurements varying Φ, the saturation value of $N_{Er,2}$ gives the maximum erbium amount that could actually be inverted for a certain excitation mechanism, i.e. N_{Er}, among the total concentration present on the sample:

$$N_{Er,2} = \frac{\sigma_{exc}\Phi}{\sigma_{exc}\Phi + 1/\tau_{21}}N_{Er} \qquad (2)$$

where σ_{exc} is the excitation cross section at a given wavelength, which has to be determined independently [7,9].

To evaluate $N_{Er,2}$ it is necessary to quantify the amount of photons emitted by the studied samples. The total photon flux emitted by the sample can be then related to $N_{Er,2}$ ($\Phi_{em} = N_{Er,2}V/\tau_{2,1rad}$). The radiative lifetime ($\tau_{2,1rad}$) is estimated to be 16 ms, which accounts for the material refractive index change with respect to the pure SiO_2 case (τ_{rad} = 18 ms), in accordance with Ref. [16]. V is the excited volume.

In Fig. 3 we present the results of this characterisation. We have plotted $N_{Er,2}$ as a function of the excitation rate $\sigma_{exc}\Phi s^{-1}$ using two sources of excitation: (i) at 975 nm that is resonant to the direct $^4I_{15/2} \rightarrow {}^4I_{11/2}$ transition (exciton formation within the Si-nc is very unlikely) and (ii) at 476 nm that is not resonant with an Er^{3+} transition but can excite the Si-nc very efficiently. Therefore, for the (i) case we are able to extract the total Er^{3+} concentration that is able to emit light, i.e. $N_{Er,act}$ and for the (ii) case the total Er^{3+} concentration that is able to emit light after an indirect excitation mechanism ($N_{Er, Si-nc}$).

With the determined values for $N_{Er,act}$ the potential gain in an amplifier will be reduced by at least a factor of 3 with respect to what would be given by the total Er^{3+} content. For sample B, this quantity can be compared to $N_{Er,Si-nc}$, revealing that about 53% of the optically active content (11% of the total content) is coupled to the Si-nc and thus invertible by indirect excitation. This means that in principle it should possible to invert the population of optically active Er^{3+} by exploiting the indirect excitation of Si-nc.

Pump and probe measurements have been performed at two different probe wavelengths in a waveguide device made of the same material as sample A. This has been done respectively at Er^{3+} emission spectrum peak (1535 nm) and almost outside the emission spectrum (1610 nm). We have excited the ions by pumping both non-resonant and resonant with Er^{3+} ions internal transi-
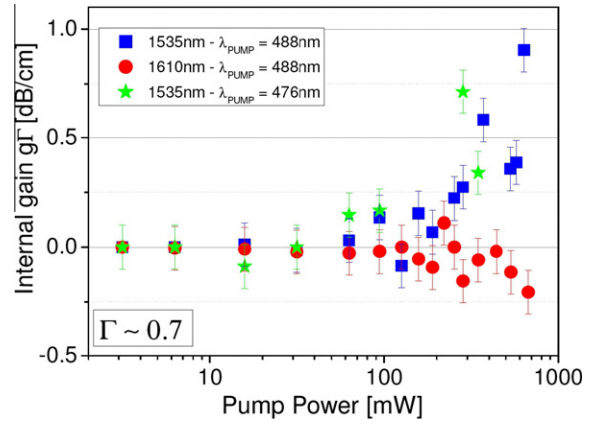
Fig. 4. $\alpha\Gamma$ measured in sample A-wg with pump & probe technique. Results for probe wavelengths tuned with the Er^{3+} emission peak (1535, black arrow in the inset) and almost outside the gain spectrum (1610 nm, red arrow in the inset) and for different excitation wavelengths are compared. (For interpretation of the references to color in this figure legend, the reader is referred to the web version of this article.)

tions (respectively λ = 476 nm and λ = 488 nm). It can be seen from Fig. 4 that the internal gain ($\alpha\Gamma$) is almost zero within the error bars in a wide range of pumping powers (from 2 to 50 mW, i.e. 10^{19} ph/cm^2 s). At higher powers g shows a positive value for the Er-gain peak wavelength probe (1535 nm) while remaining zero for the probe wavelength outside the Er emission peak (1610 nm).

Considering a confinement factor of about 0.7, at medium photon fluxes we have measured a maximum internal gain of about 1 dB/cm, i.e. a reduction of 2 dB/cm of the initial absorption losses. By comparing this value with the absorption coefficient at 1535 nm (about 4 dB/cm) [9] we were able to invert about 25% of the Er^{3+} that was absorbing, though we were expecting about 53% from quantification measurements. Therefore, even taking into account the limitations of the presented results it appears that there is a sizeable Er^{3+} fraction that is not optically active while, on the contrary, it can absorb the light that should be amplified. One possible explanation would be that this population suffers from local concentration quenching effects (in a way that the excitation can migrate from one ion to another until it encounters a quenching centre where a local phonon or deformation can deactivate the excitation). Indeed, such an agglomeration has been reported for ion implanted Si rich SiO_2 co-doped with Er^{3+} ions by means of energy-filtered transmission electron microscopy and high annular angle dark field [17].

4. Conclusions

In this work we have shown different studies that provide a wide overview of Si-nc coupled to Er^{3+} ions in a SiO_2 matrix. On the one hand, we have derived a model for the Si-nc/Er^{3+} interaction dynamics that can coherently account for several experimental facts derived from CW and TR visible and infrared PL measurements.

We performed a quantitative study of the Er^{3+} maximum concentrations able to emit light by direct or indirect excitation means and compared them with the total content present in the sample. In particular, we show that $N_{Er,Si-nc}$ is lower than N_{Er}, which are both lower than the overall Er content present in the matrix.

Moreover, from pump and probe measurements on a waveguide device we infer that the relative content that could be inverted seems to be lower than the Er^{3+} content that is indeed absorbing. Those are results that may impact in the potential performances of this material for amplification purposes.
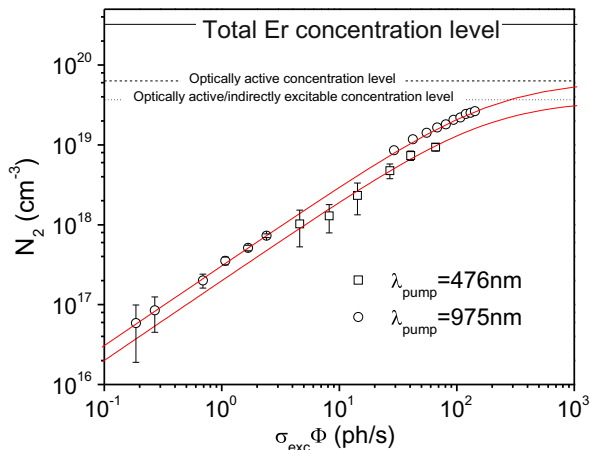

Fig. 3. $N_{Er,2}$ as a function of $\sigma_{exc}\Phi$ (in log–log scale) for sample A. Two pumping wavelengths have been used: 975 nm (circles) and 476 nm (squares). The respective fits using Eq. (2) are also shown. The different achievable concentration levels are also represented as horizontal lines.

Acknowledgements

References

[1] A.J. Kenyon, P.F. Trwoga, M. Federighi, C.W. Pitt, J. Phys.: Condens. Matter 6 (1994) L319–L324.
[2] M. Wojdak, M. Klik, M. Forcales, O.B. Gusev, T. Gregorkiewicz, D. Pacifici, G. Franzò, F. Priolo, F. Iacona, Phys. Rev. B 69 (2004) 233315.
[3] P.G. Kik, A. Polman, J. Appl. Phys. 88 (2000) 1992.
[4] B. Garrido, C. García, S.-Y. Seo, P. Pellegrino, D. Navarro-Urrios, N. Daldosso, L. Pavesi, F. Gourbilleau, R. Rizk, Phys. Rev. B 76 (2007) 245308.
[5] I. Izeddin, A.S. Moskalenko, I.N. Yassievich, M. Fujii, T. Gregorkiewicz, Phys. Rev. Lett. 97 (2006) 207401.
[6] C.J. Oton, W.H. Loh, A.J. Kenyon, Appl. Phys. Lett. 89 (2006) 031116.
[7] D. Navarro-Urrios, Y. Lebour, O. Jambois, B. Garrido, A. Pitanti, N. Daldosso, L. Pavesi, J. Cardin, K. Hijazi, L. Khomenkova, F. Gourbilleau, R. Rizk, J. Appl. Phys. 106 (2009) 093107.
[8] K. Hijazi, L. Khomenkova, J. Cardin, F. Gourbilleau, R. Rizk, Physica E 41 (6) (2009) 1067.
[9] D. Navarro-Urrios, A. Pitanti, N. Daldosso, F. Gourbilleau, L. Khomenkova, R. Rizk, L. Pavesi, Physica E 41 (2009) 1029.
[10] D. Navarro-Urrios, A. Pitanti, N. Daldosso, F. Gourbilleau, R. Rizk, B. Garrido, L. Pavesi, Phys. Rev. B 79 (2009) 193312.
[11] O. Savchyn, R.M. Todi, K.R. Coffey, P.G. Kik, Appl. Phys. Lett. 93 (2008) 233120.
[12] R. M'ghäieth, H. Maâref, I. Mihalcescu, J.C. Vial, Phys. Rev. B 60 (1999) 4450.
[13] F. Gourbilleau, R. Madelon, C. Dufour, R. Rizk, Opt. Mater. 27 (2005) 868.
[14] I. Izeddin, M.A.J. Klik, N.Q. Vinh, M.S. Bresler, T. Gregorkiewicz, Phys. Rev. Lett. 99 (2007) 077401.
[15] A. Pitanti, D. Navarro-Urrios, N. Prtljaga, N. Daldosso, F. Gourbilleau, R. Rizk, B. Garrido, L. Pavesi, J. Appl. Phys. 108 (2010) 053518.
[16] M.J.A. de Dood, L.H. Slooff, A. Polman, A. Moroz, A. van Blaarderen, Phys. Rev. A 64 (2001) 033807.
[17] P. Pellegrino, B. Garrido, J. Arbiol, C. Garcia, Y. Lebour, J.R. Morante, Appl. Phys. Lett. 88 (2006) 121915.